

Decomposition of Spontaneous Brain Activity into Distinct fMRI Co-activation Patterns

Xiao Liu*, Catie Chang, and Jeff H. Duyn

Supplementary Figures 1–8

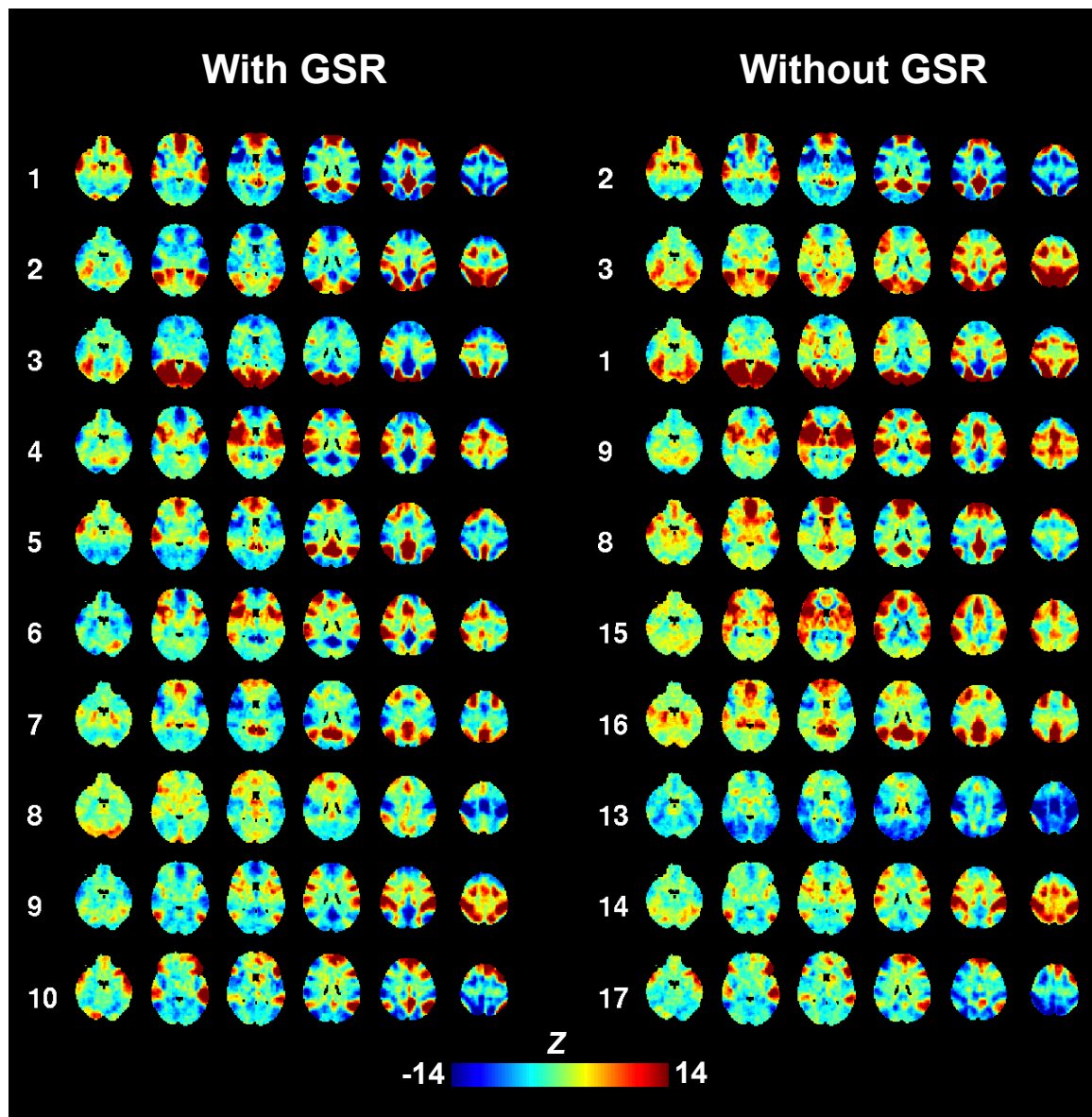


Fig. S1. Effects of global signal regression (GSR) on CAPs. The CAPs 1–10 identified with using GSR are largely similar to corresponding CAPs extracted without using the GSR, except that some CAPs show a global shift of the distribution of their map statistics toward more positive or negative values.

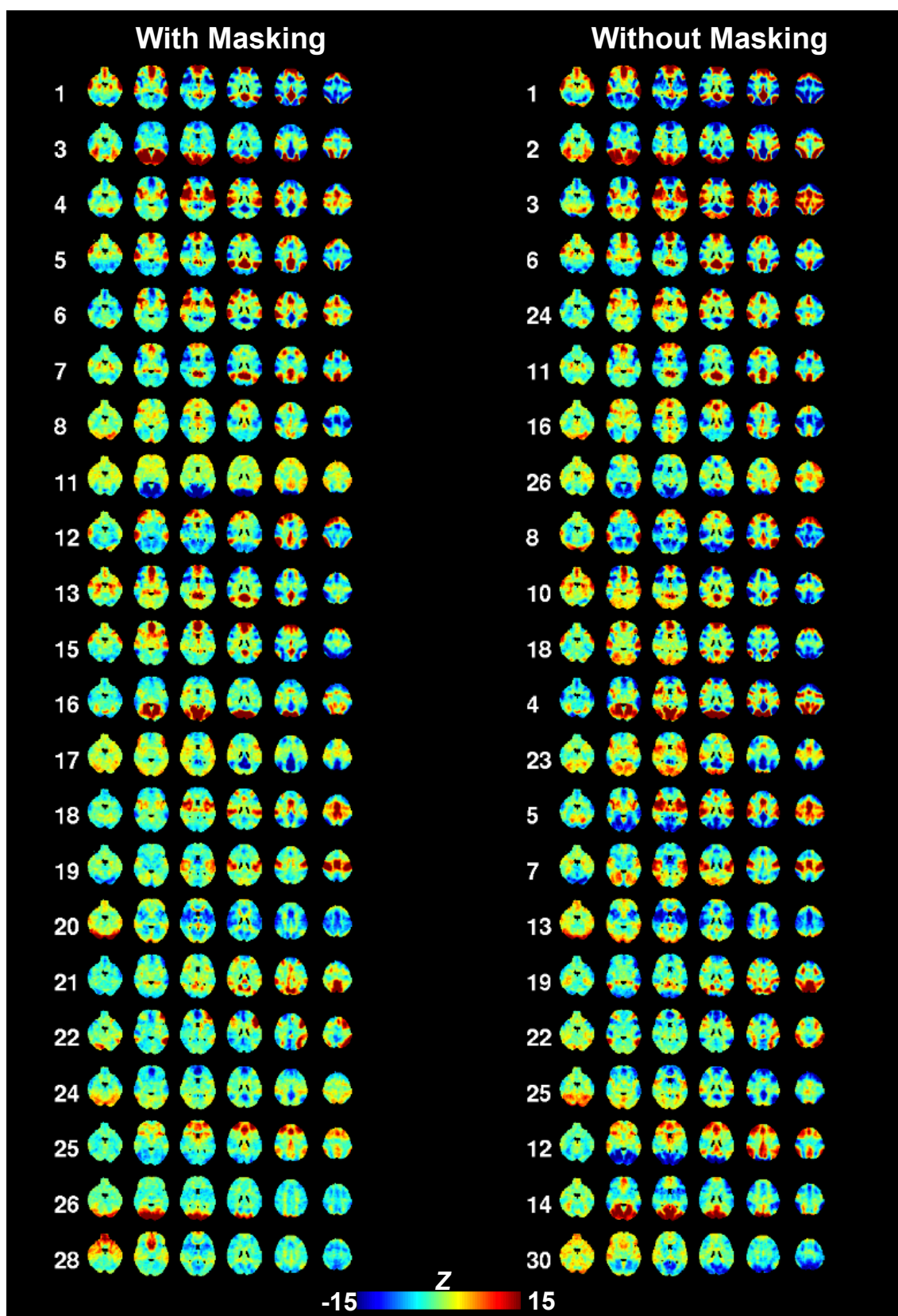
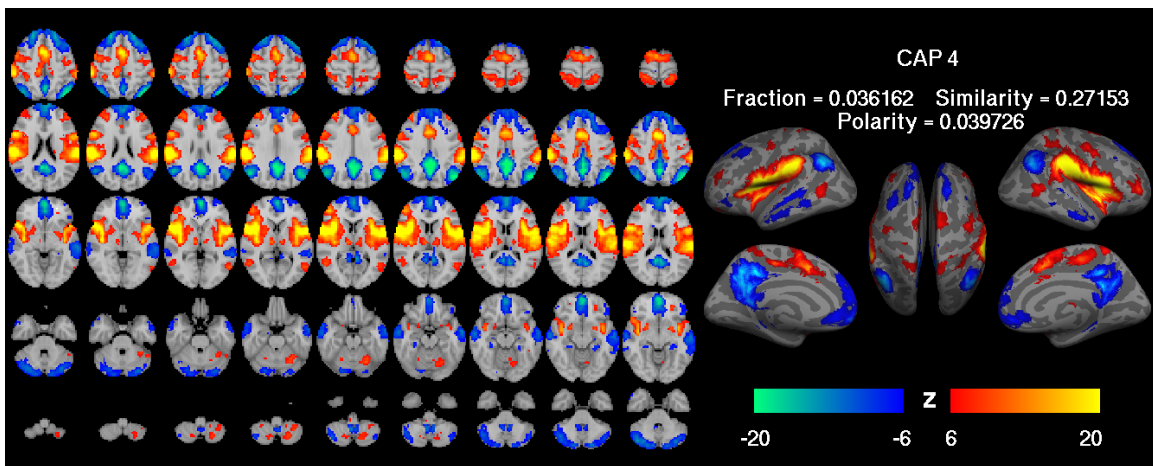
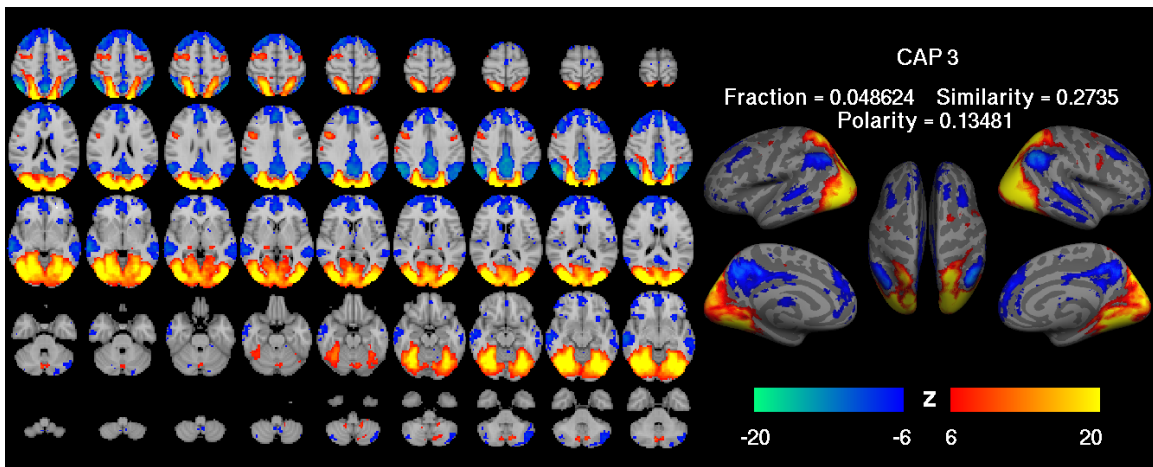
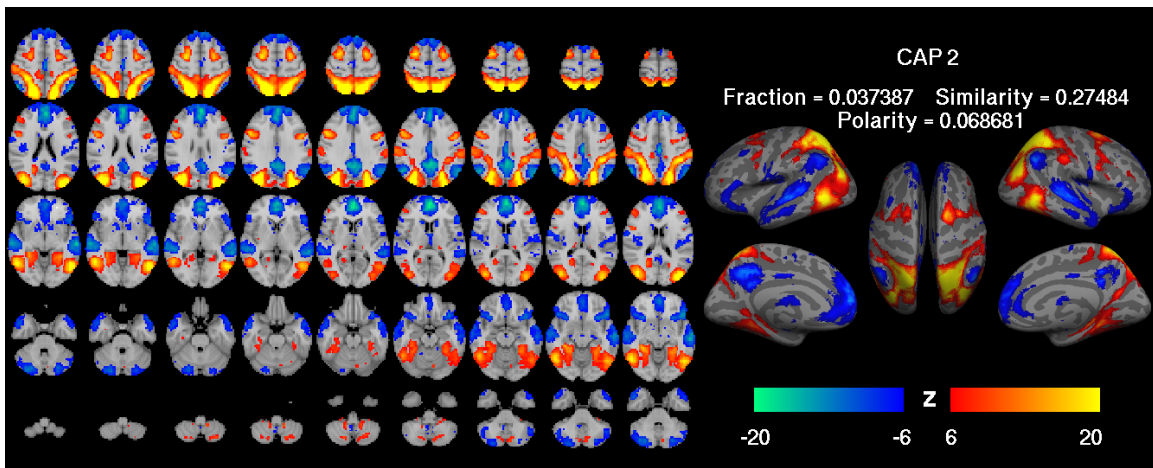
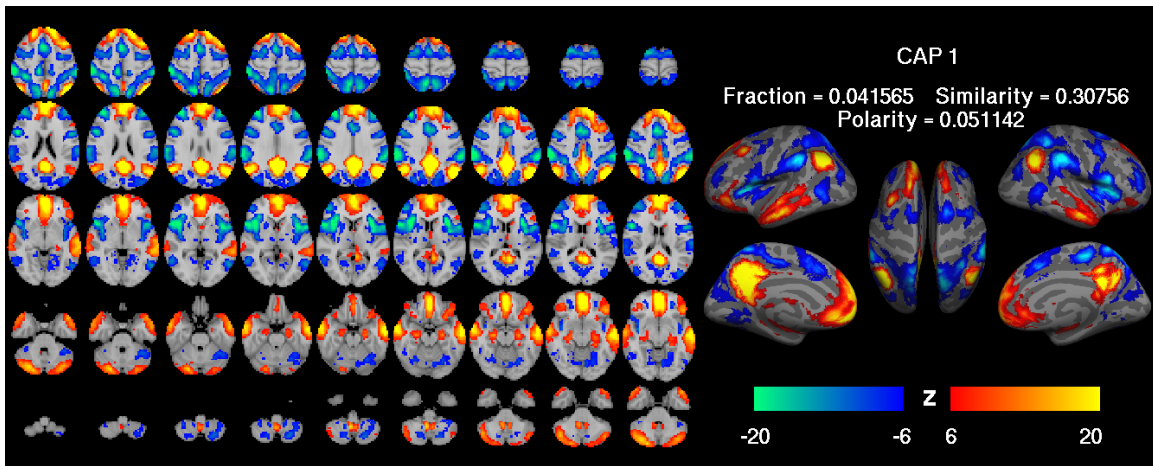
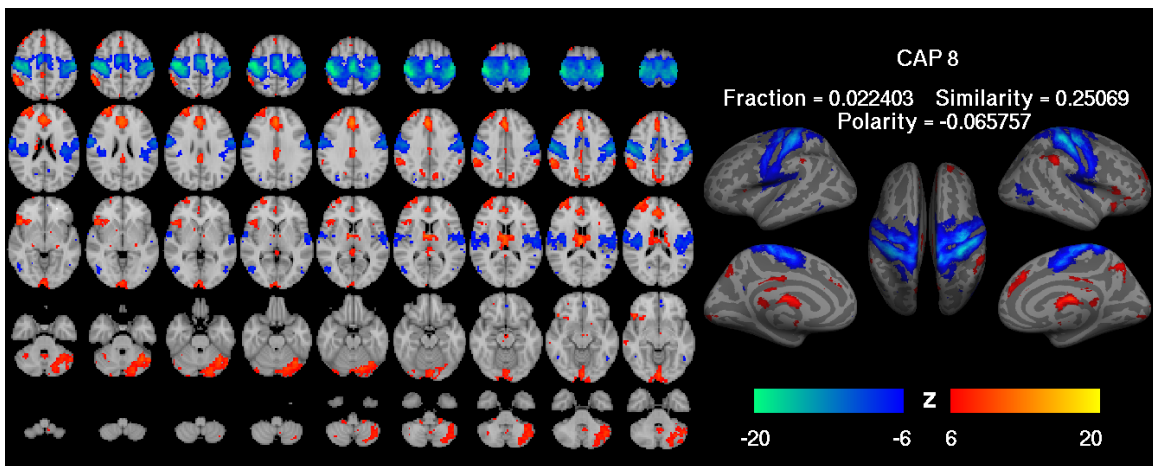
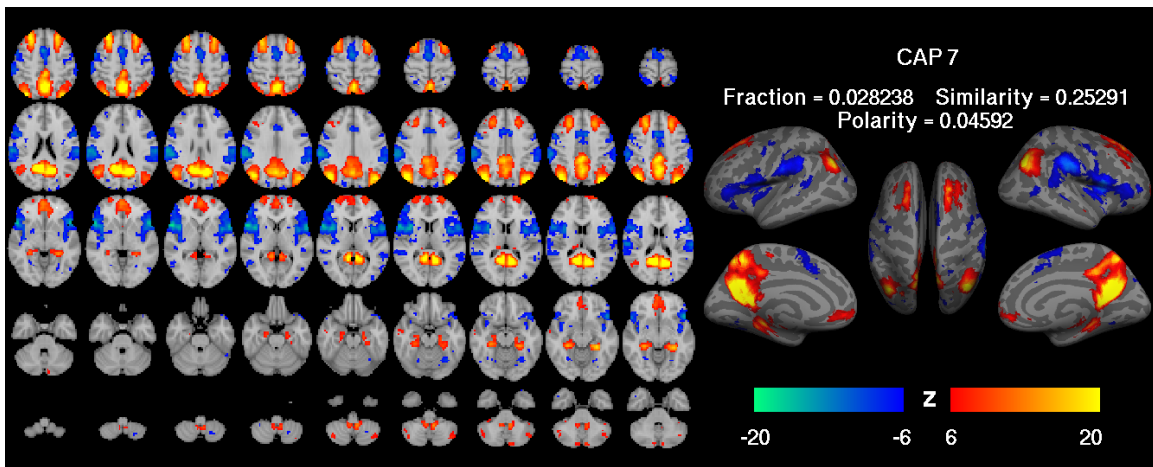
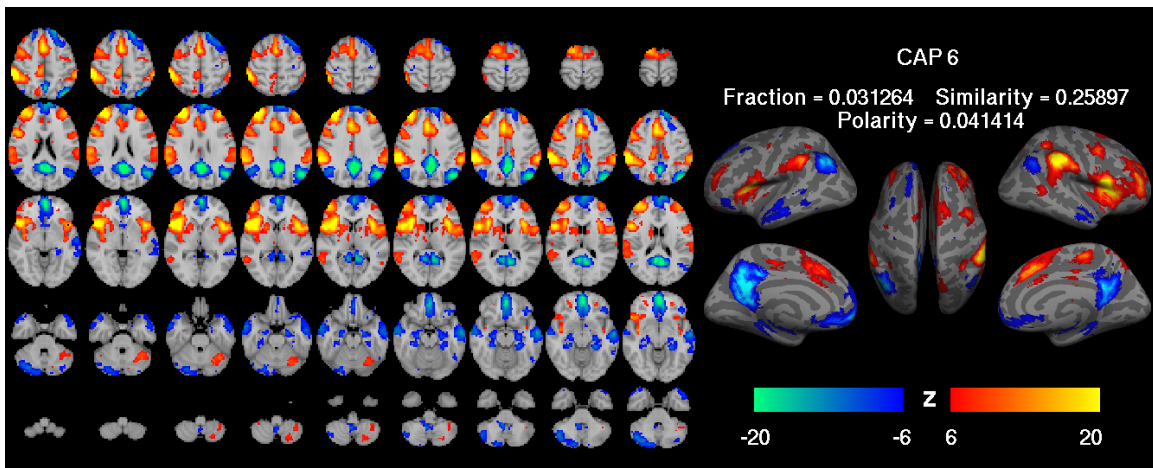
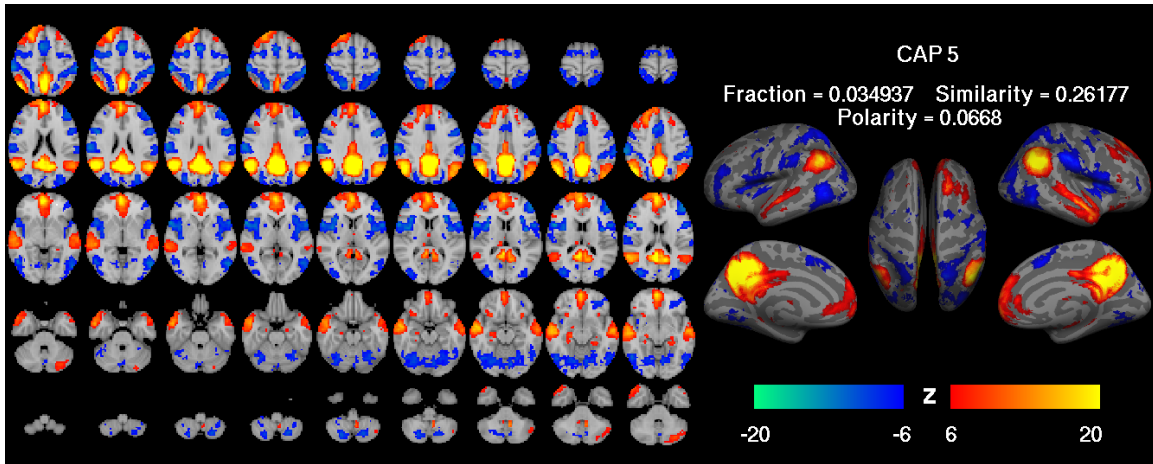
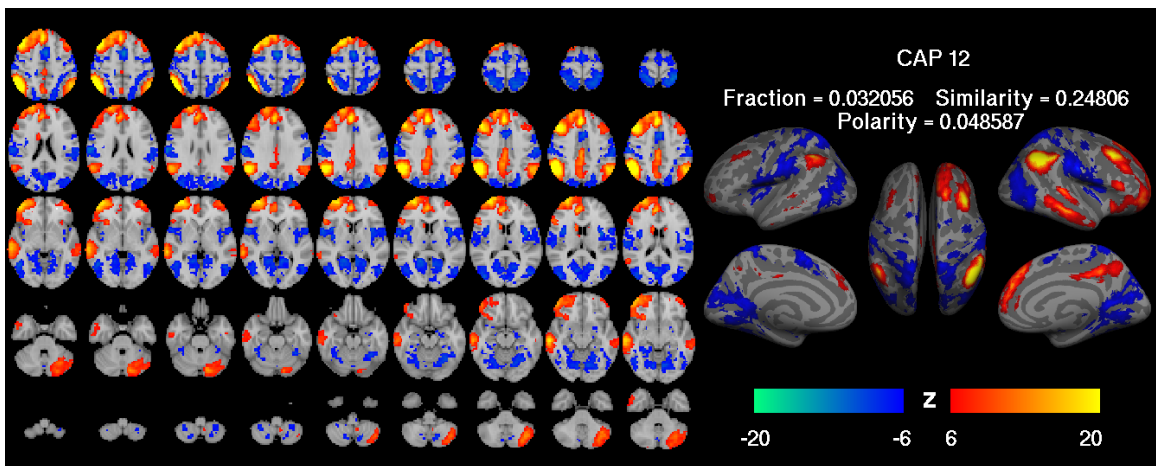
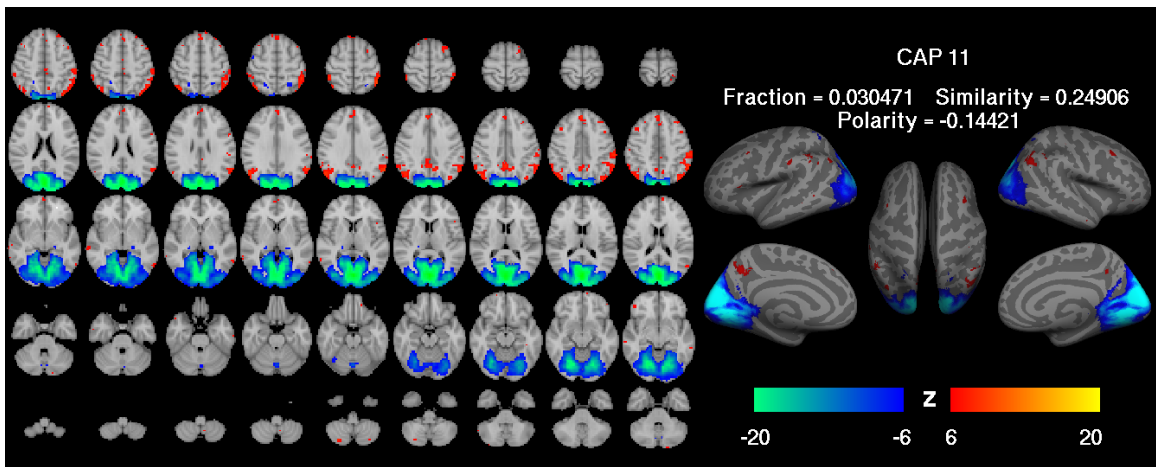
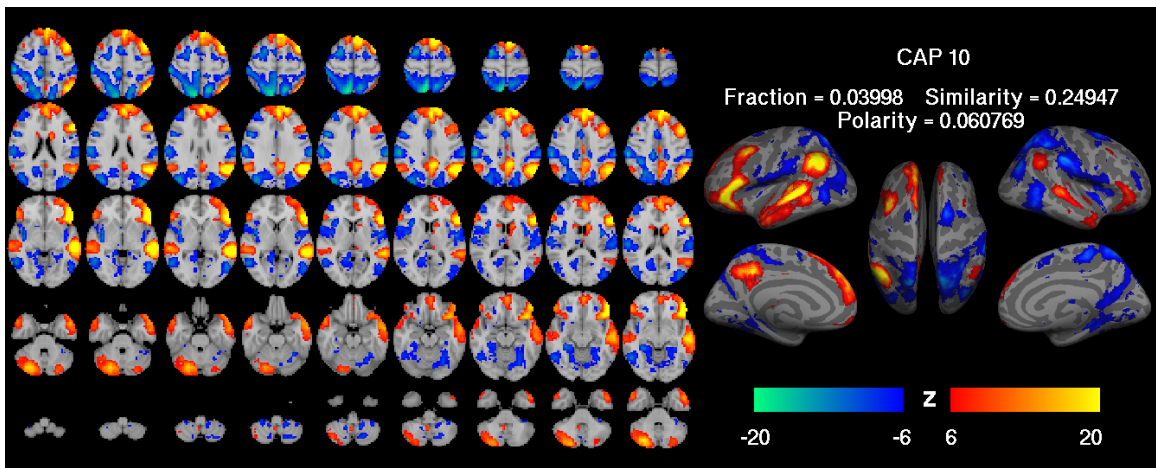
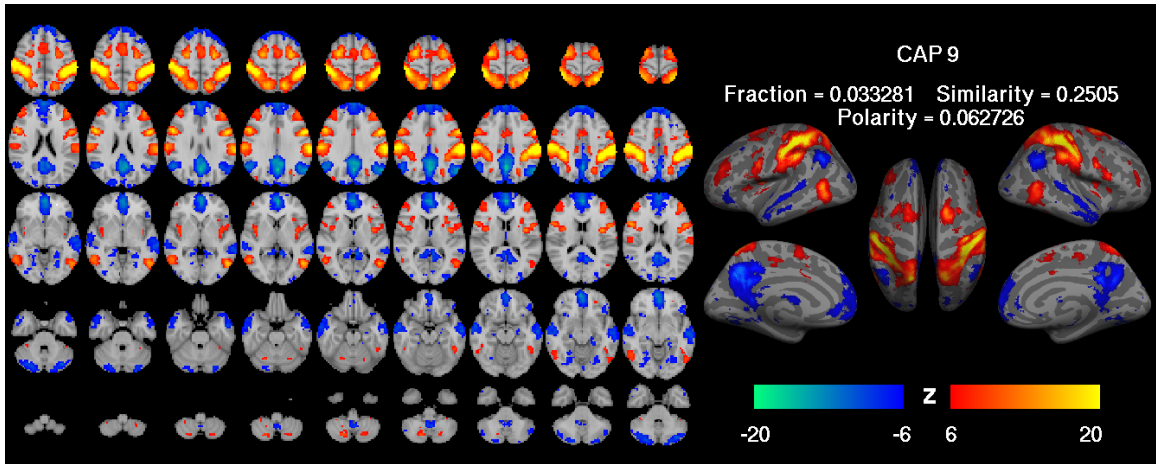
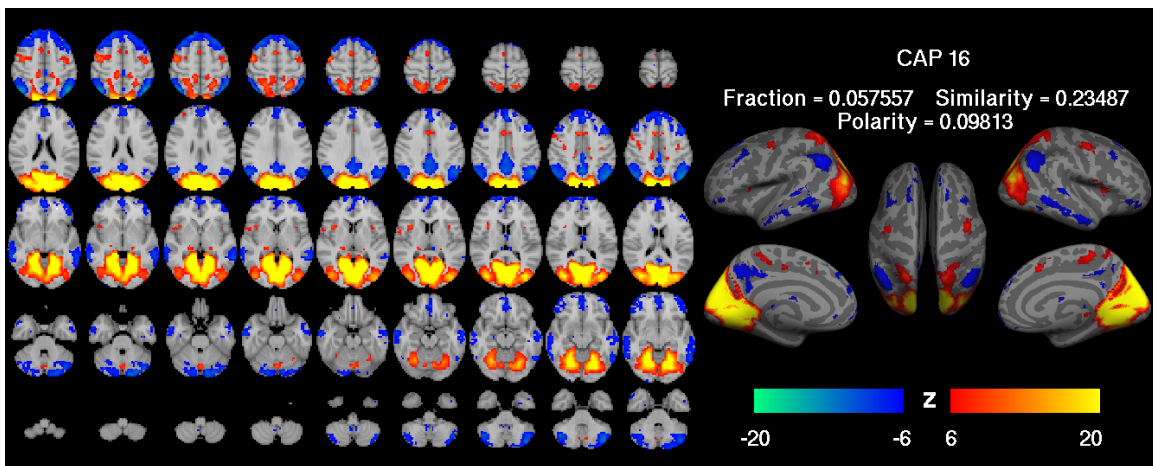
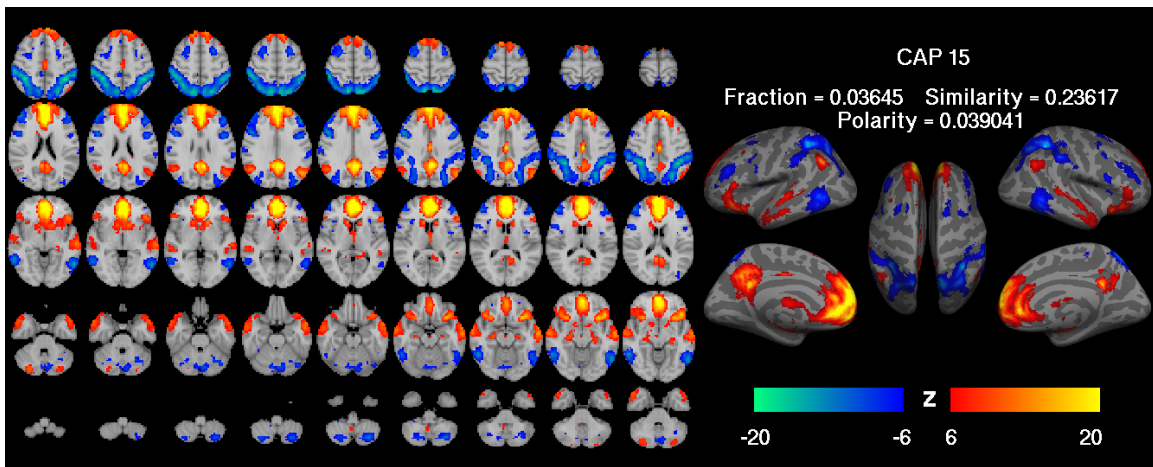
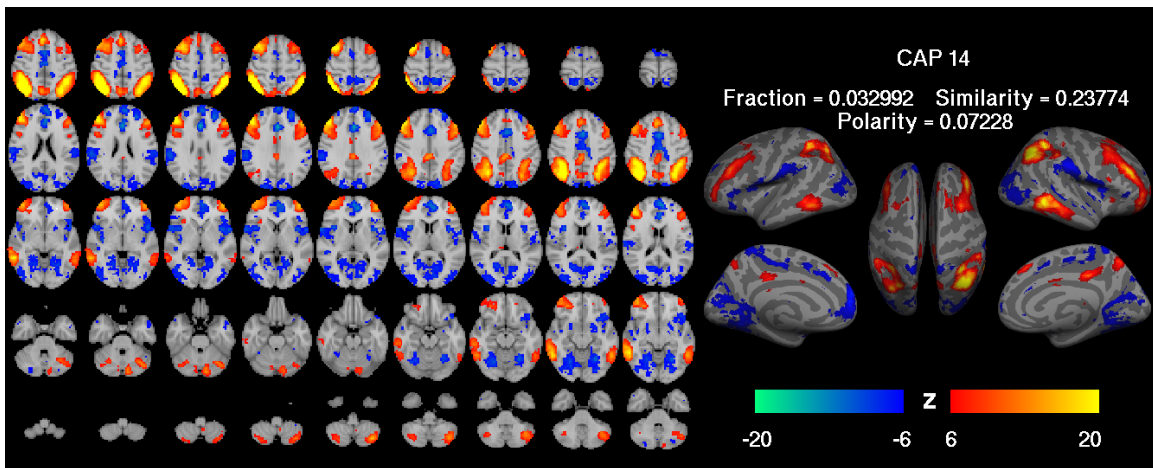
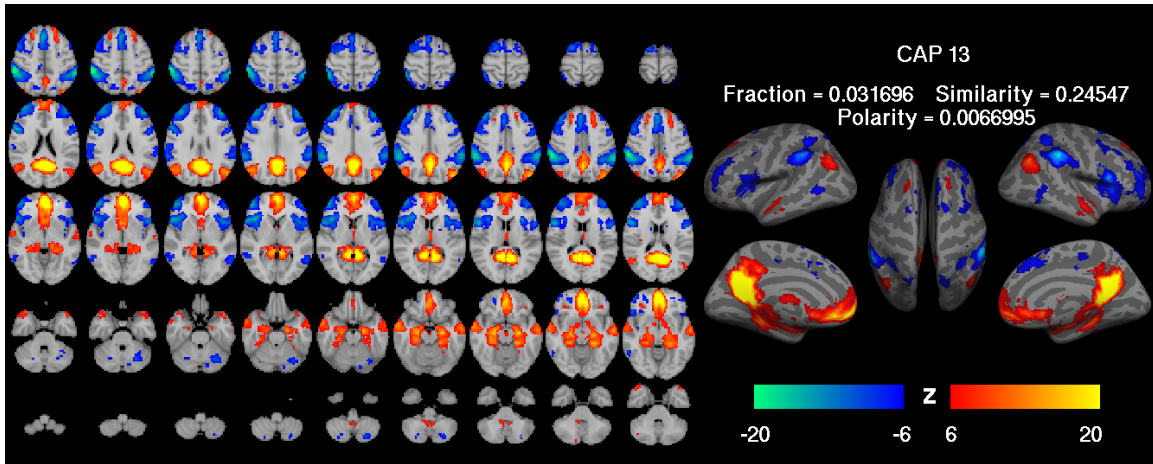


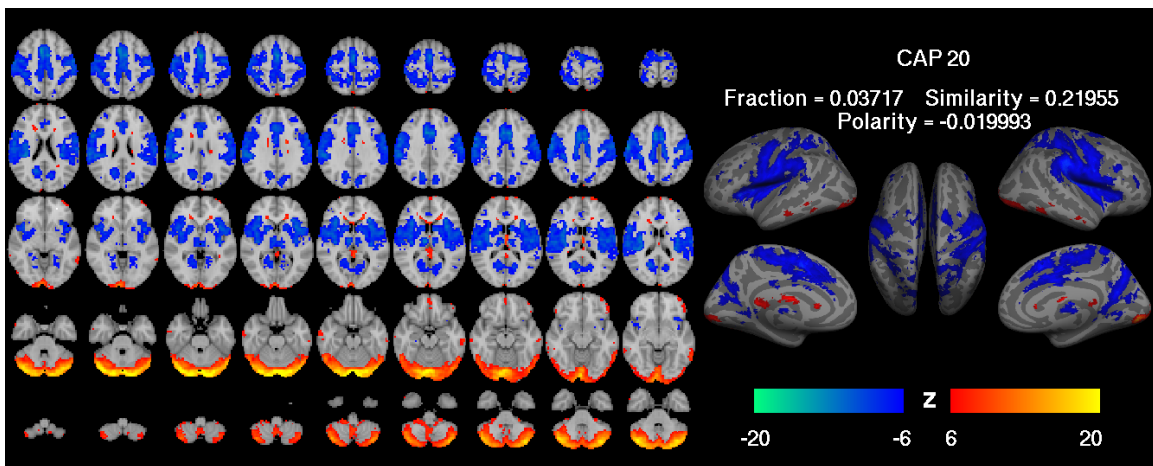
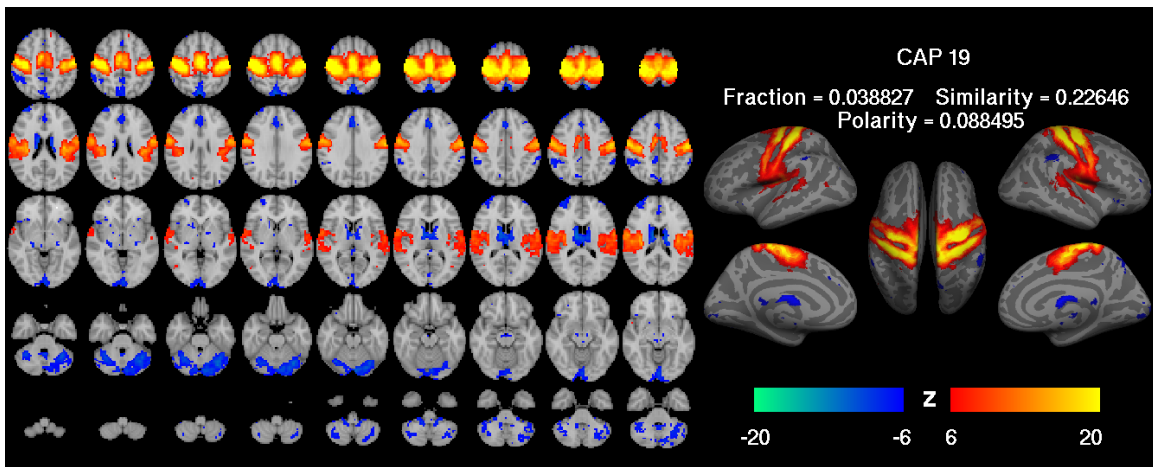
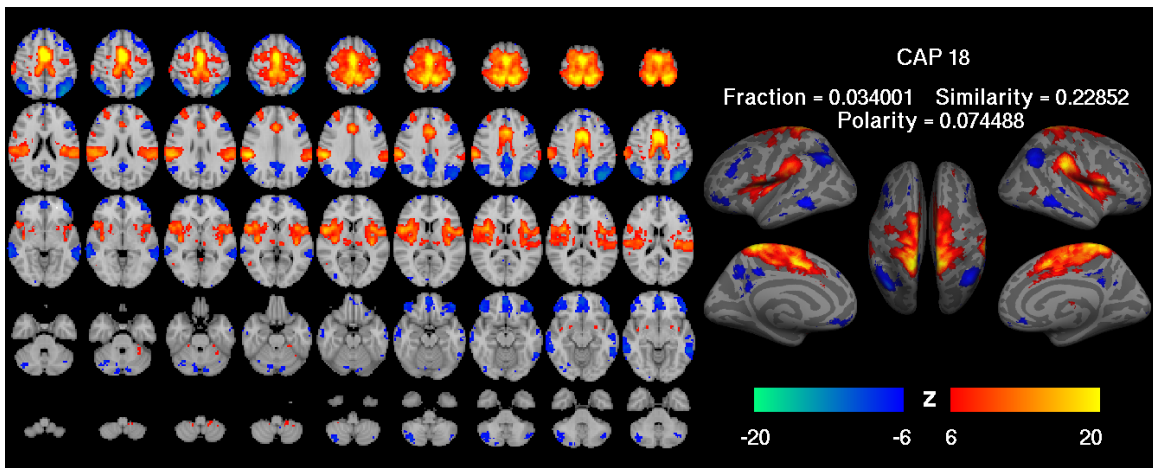
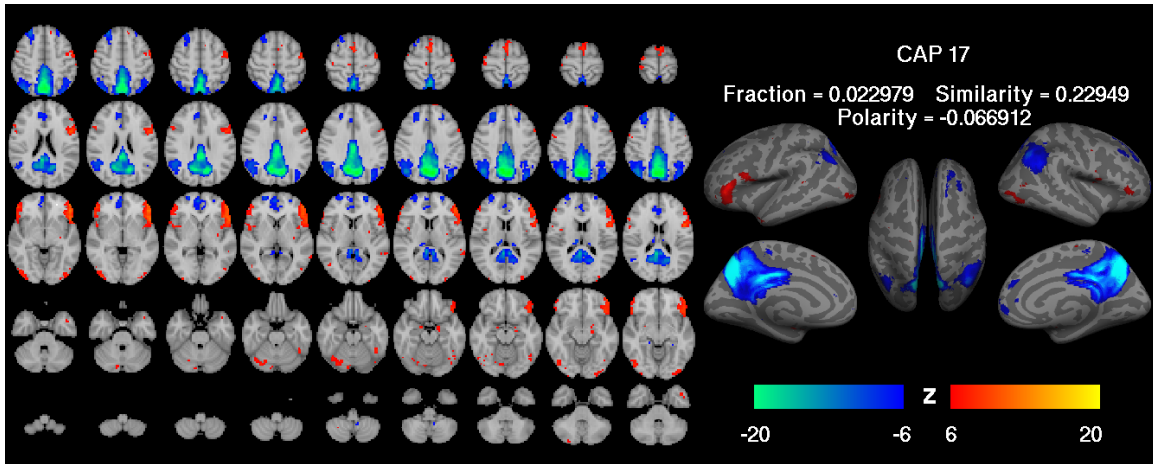
Fig. S2. CAPs obtained with (left) and without (right) noise masking procedure. Only subtle difference are observed between these condition, suggesting noise masking is not critical.

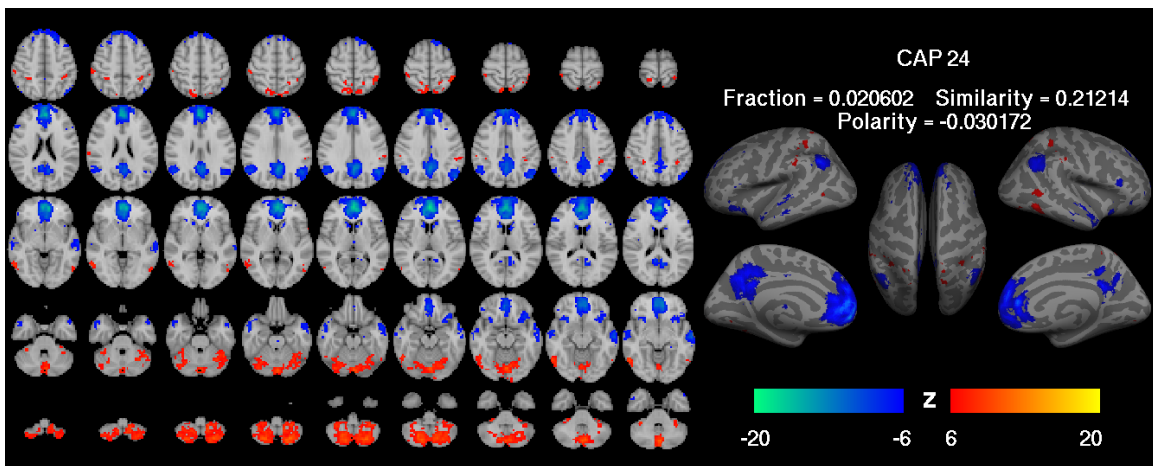
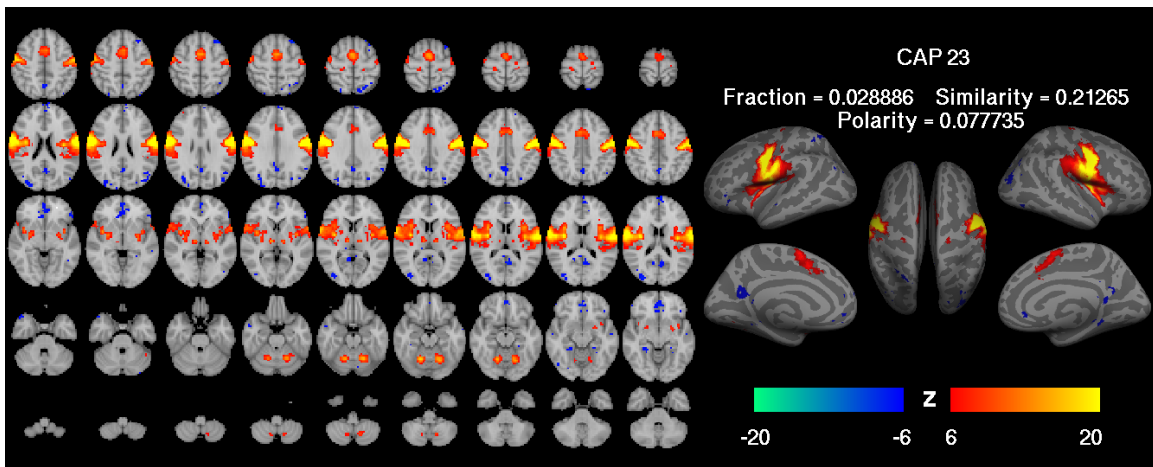
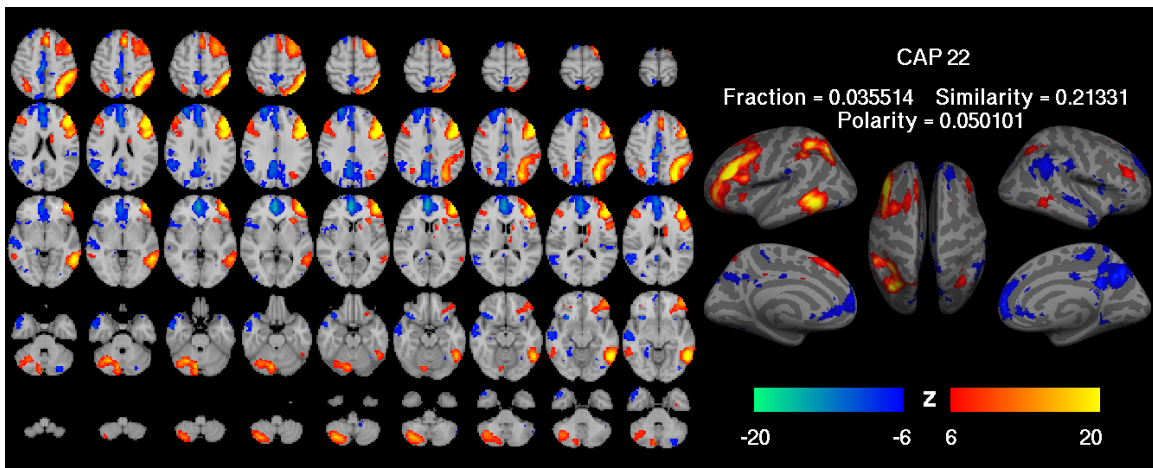
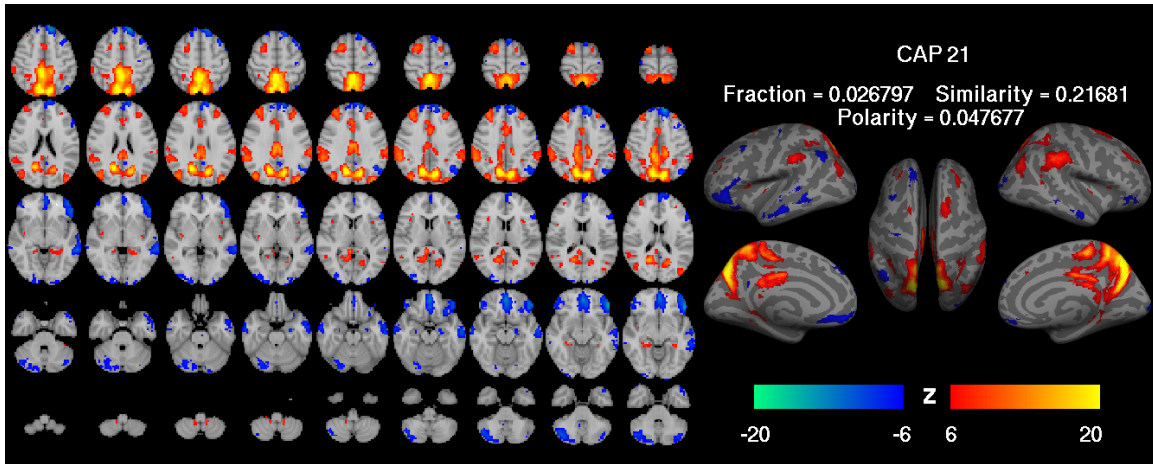


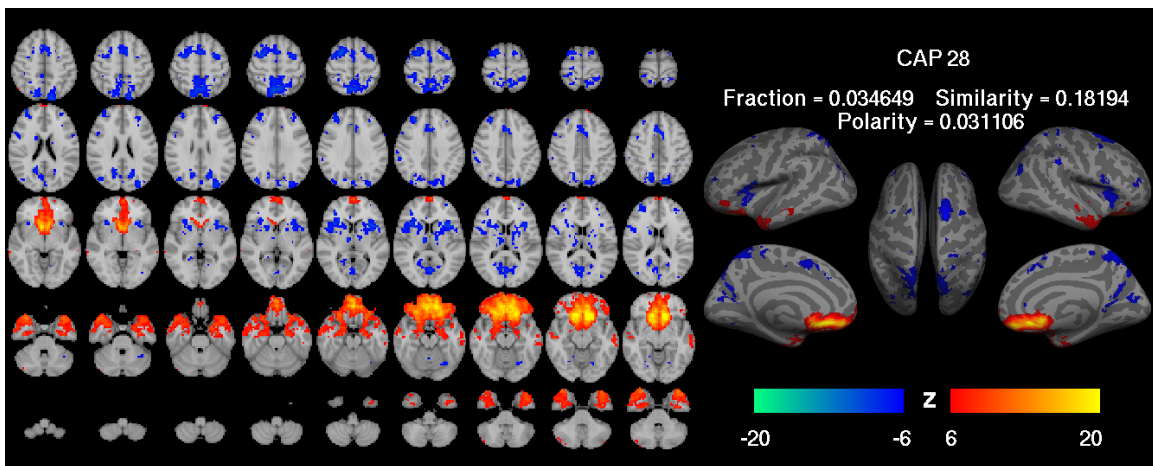
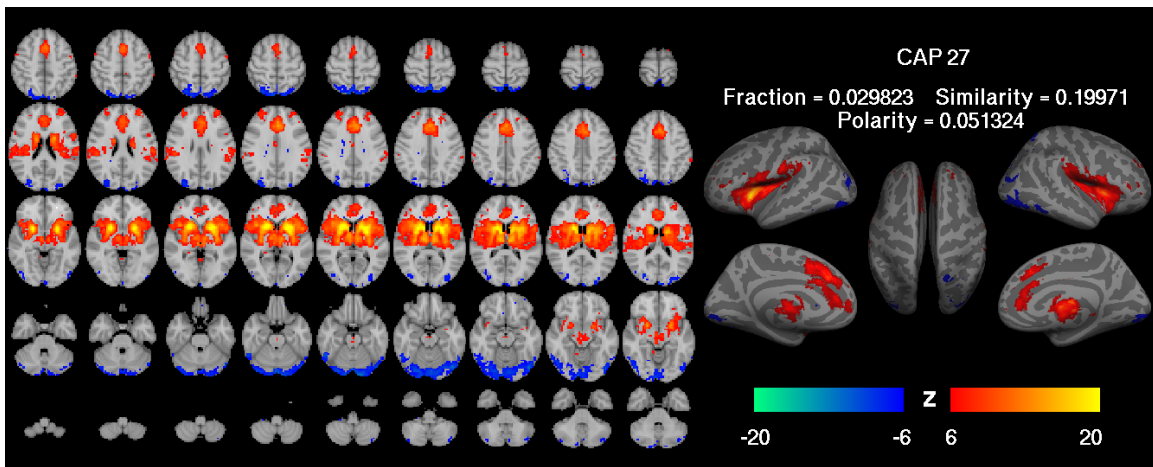
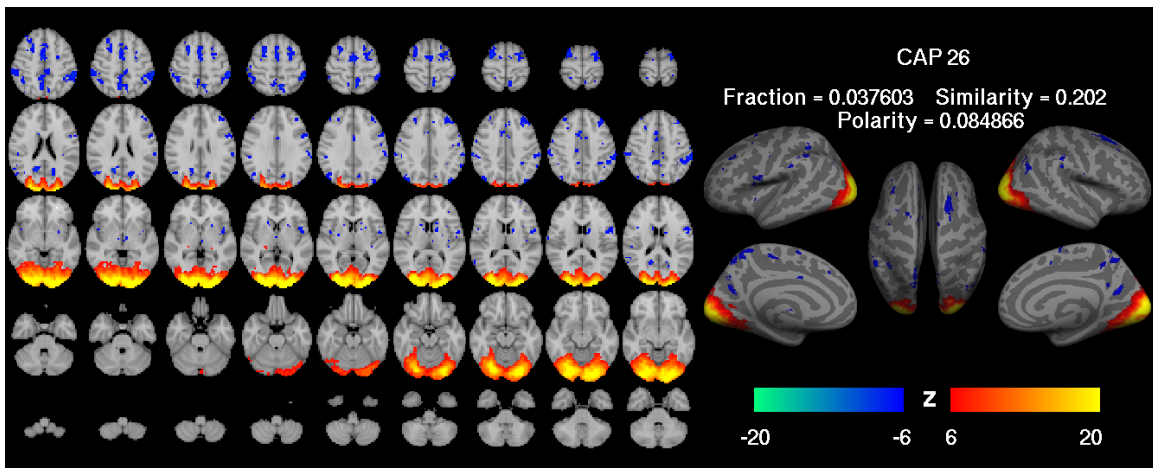
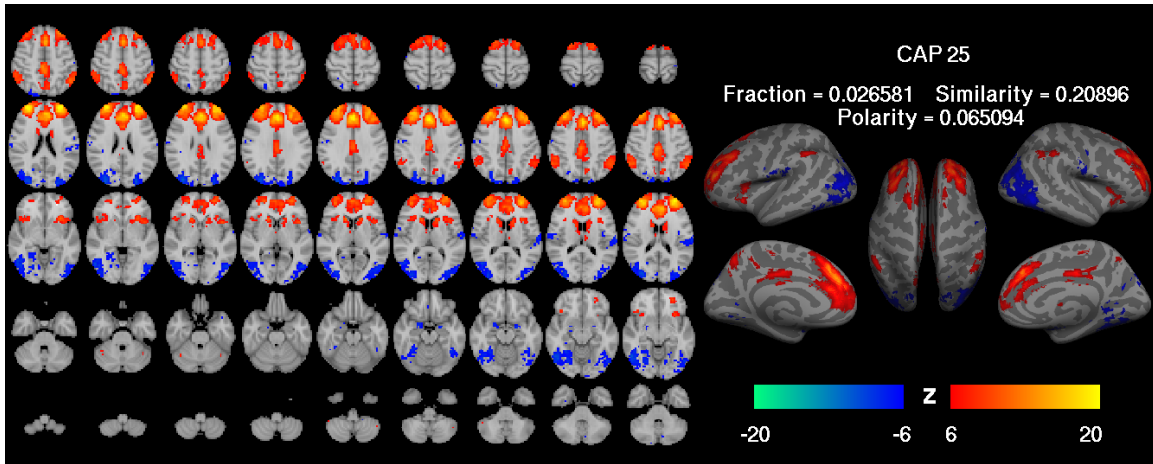












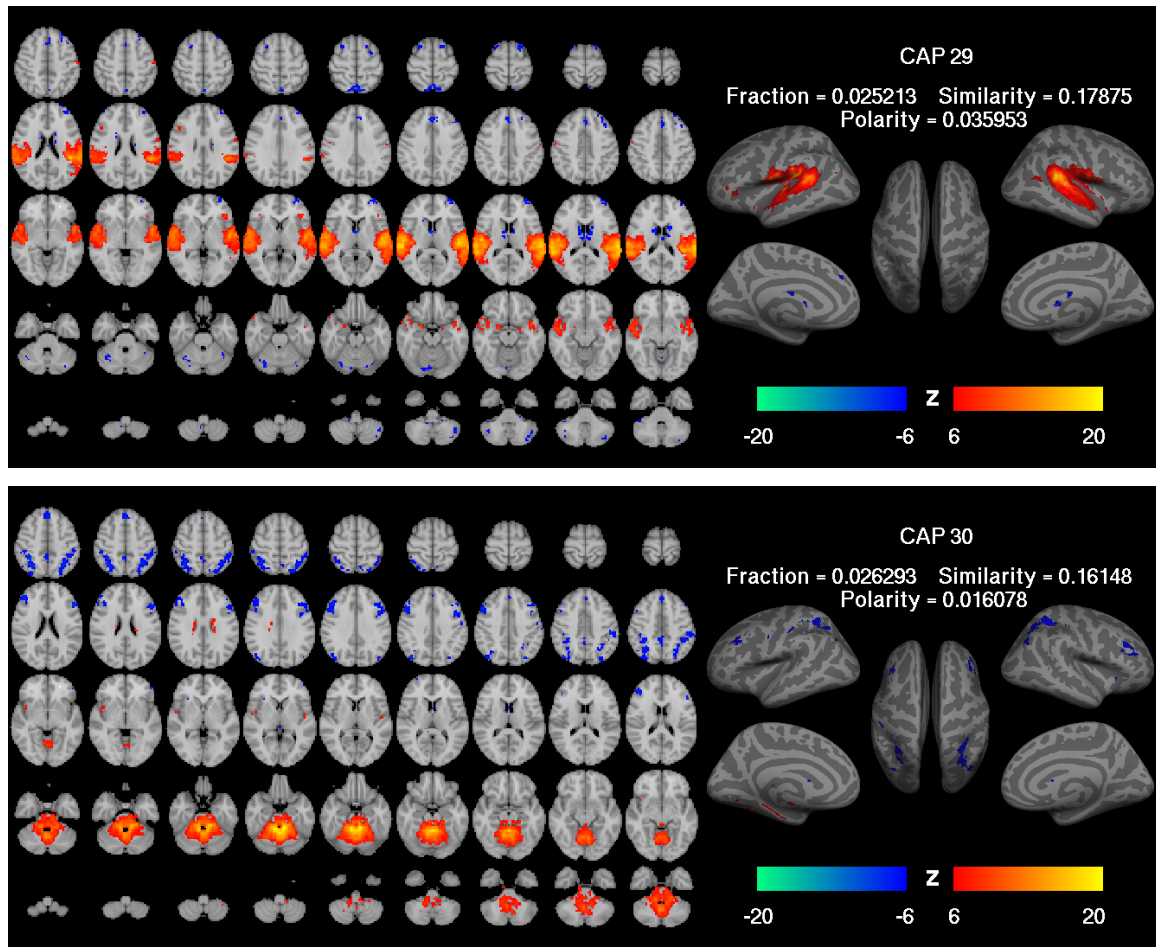


Fig. S3. Detailed information of 30 CAPs extracted with the proposed method. Each CAP was overlaid on the 152-MNI template in 2D slices (upper) and 3D surface (lower) with their occurrence rate, with-group similarity, and polarity showing in the middle. The color encoding of z-score is identical to that in Figure 3 ($6 < |z| < 20$). Many of these CAPs resembled RSNs extracted with conventional analysis, suggesting network activity in the DMN (CAPs 1,7,12,15), sensory regions with or without DMN involvement (CAPs 2,3,4,6,9 and CAPs 16,19,23,26,29 respectively).

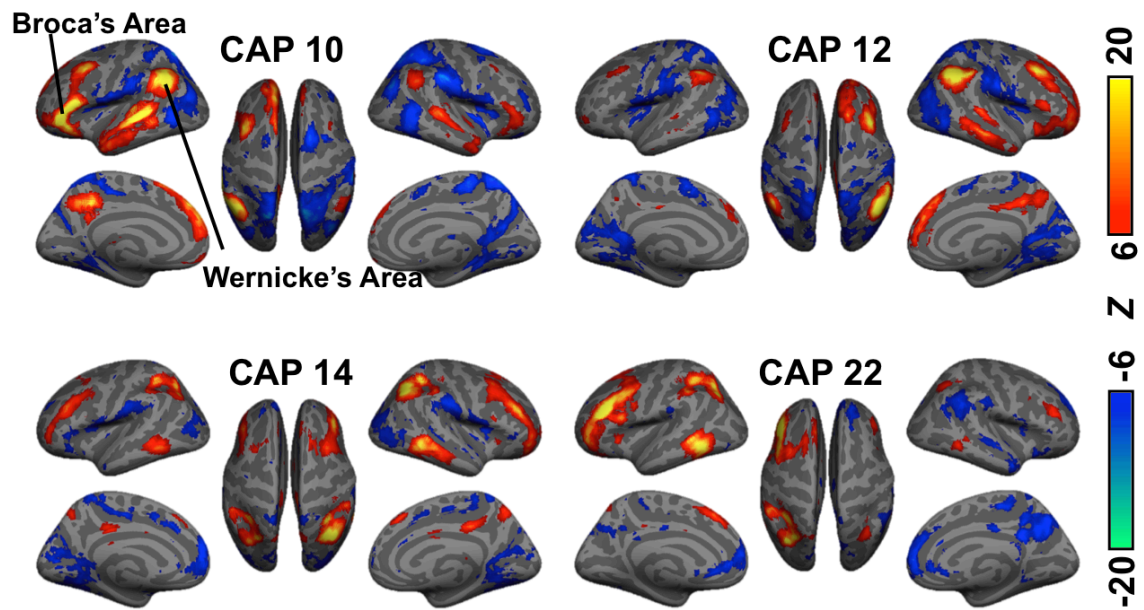


Fig. S4. Several CAPs show highly lateralized patterns. For example, CAP 10 has dominant activation at language-related areas in the left hemisphere, and has a contralateral analogue in CAP 12. Similarly, CAP 22 is lateralized and has its contralateral analogue (although somewhat weakened) in CAP 24. Also worth noting is the fact that the activity patterns in these CAPs often show very sharp transition across the brain's midline, particularly around the PCC and precuneus (Fig. S1, CAPs 10, 12, and 22).

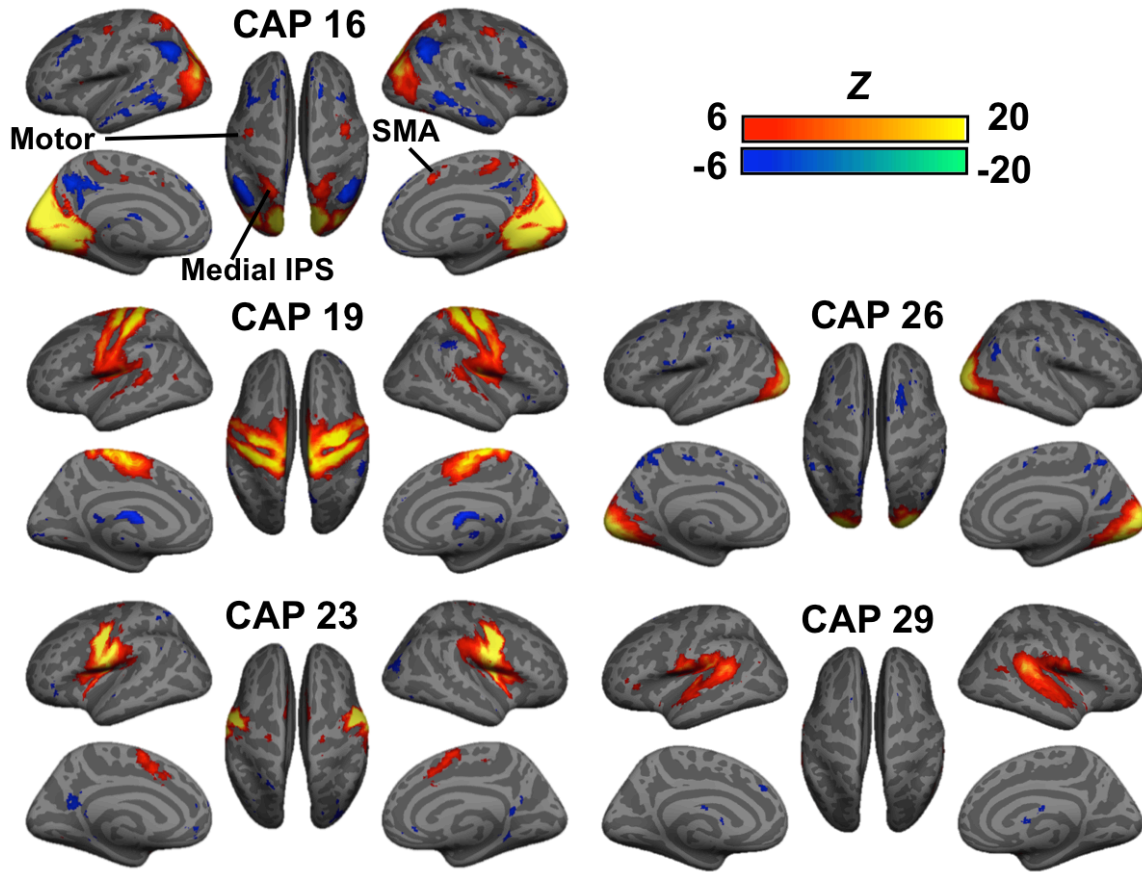


Fig. S5. A number of CAPs exhibited strong activity in primary sensory regions, including the peripheral visual (CAP 16), central visual (CAP 26), auditory (CAP 29), and sensorimotor cortices (CAPs 19 and 23). Of the latter, CAP 19 mainly covers the posterior SMA and the medial sensorimotor regions responsible for lower body parts, while CAP 23 encompasses the anterior SMA and the most lateral sensorimotor regions controlling facial muscles) cortices. While the co-activations in these sensory CAPs are mostly local, some of them show focal structures co-activated in remote brain regions. For example, the visual-related CAP 16 shows very specific co-activations at the motor cortex, SMA, and medial IPS.

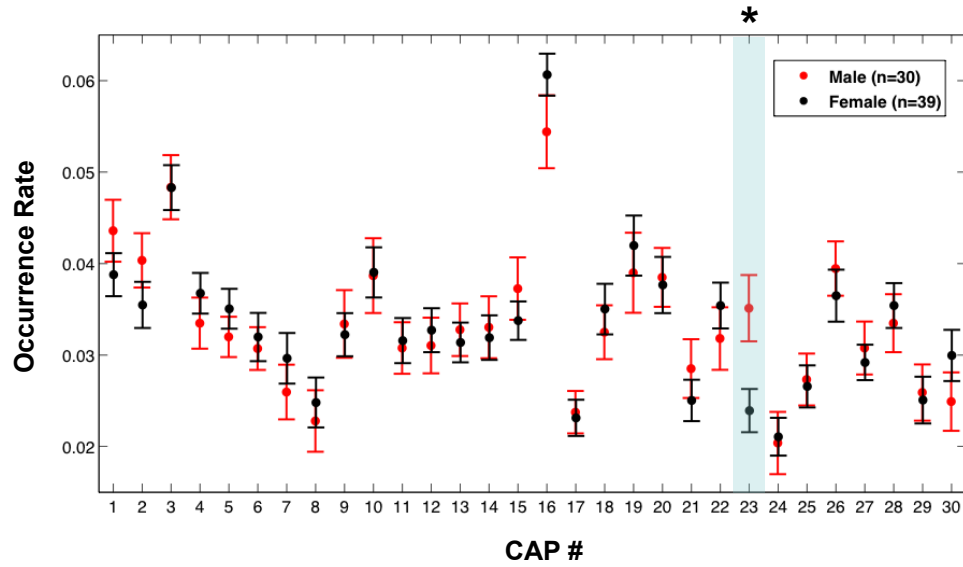
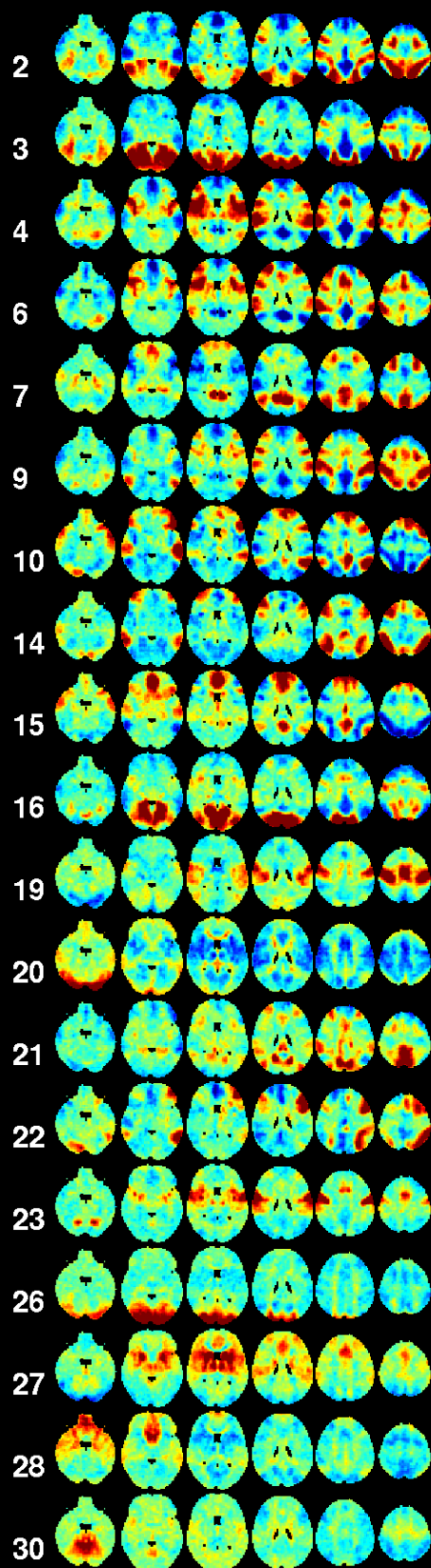


Fig. S6. Occurrence rates of the CAPs in a subgroup of males and females with comparable motions. Error bars represent the standard error across participants. The asterisk indicates CAPs showing a significant difference in their occurrence ($p < 0.01$ with Bonferroni correction, permutation test) between these two groups.

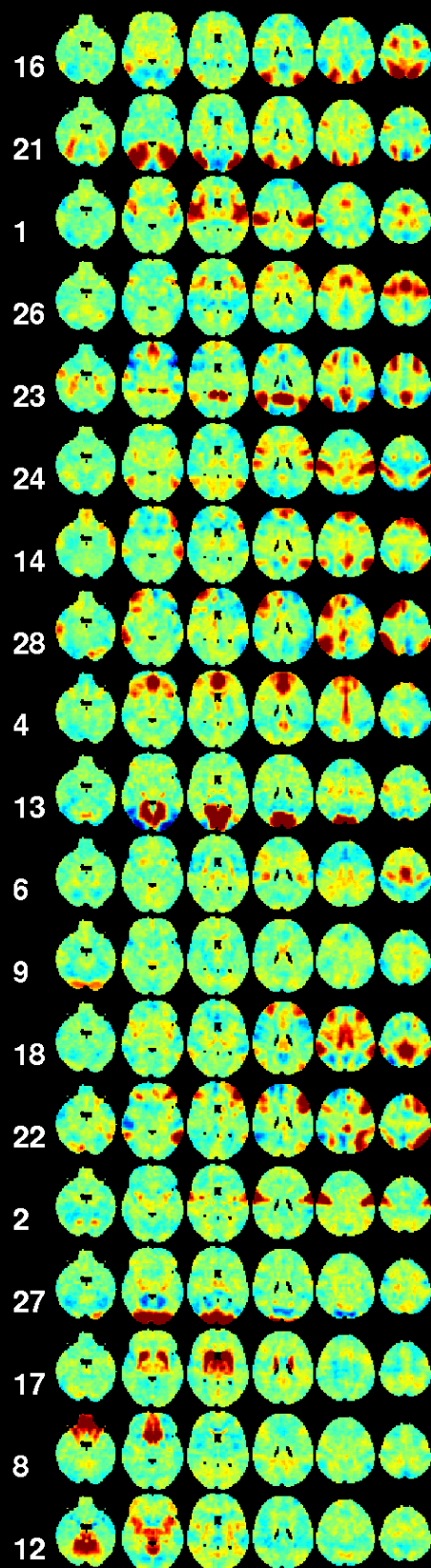
CAPs



-15 15

Z

ICs



-8 8

Fig. S7. 19 matched CAP–IC pairs, defined as those having highest spatial correlation to each other among their own categories. Although some of the CAPs show a coarse similarity, close inspection revealed distinct differences. For example, CAP 23 and IC 2 both cover sensorimotor areas, but the co-activation in supplementary motor area (SMA) is strong in CAP 23 but absent in IC 2. In addition, many CAPs show strong negative statistics indicating de-activations in a wide range of regions, while negative statistics in the ICs are generally much weaker.

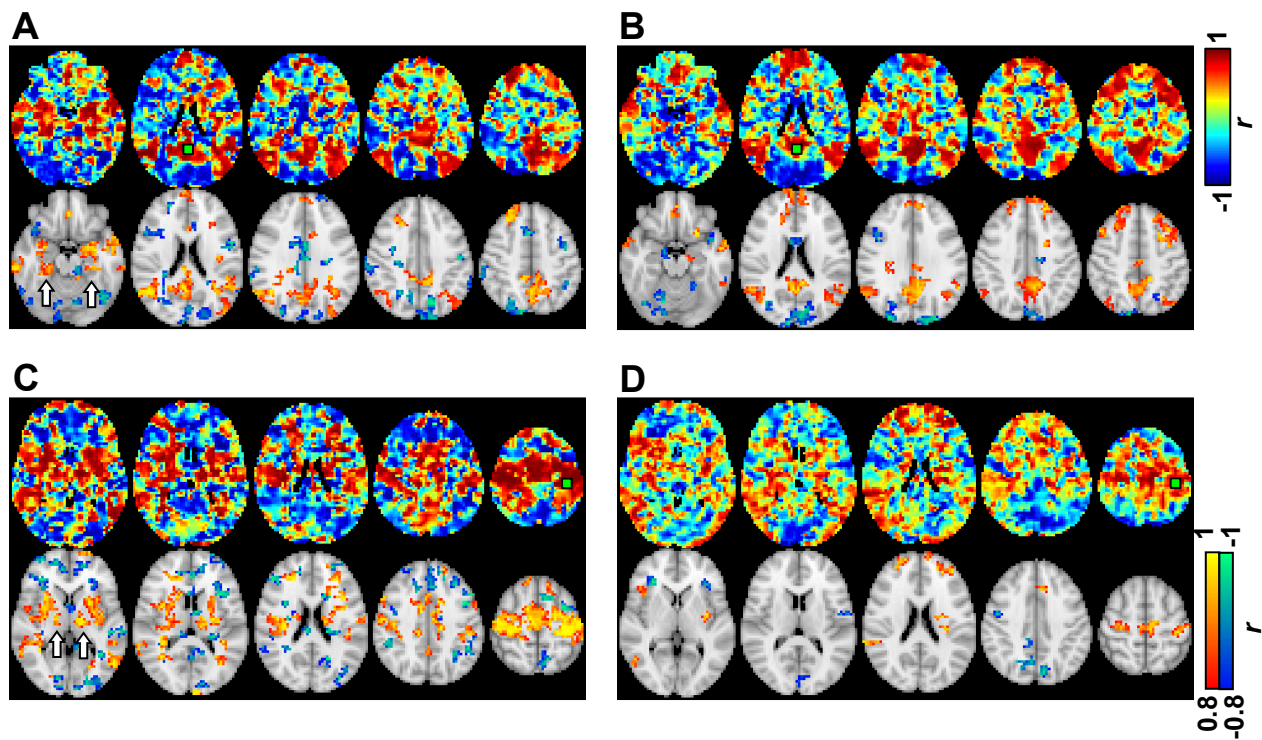


Fig. S8. PCC-seeded correlation maps from a representative subject (the same one in Figure 1) using a short sliding window (16.1-sec, 7 time points). The sliding window was centered at T11 (A), T12 (B), T3 (C), and T9 (D) shown in Figure 1, respectively. Each correlation map is shown without (upper row) and with (lower row) being overlaid on corresponding anatomical images.

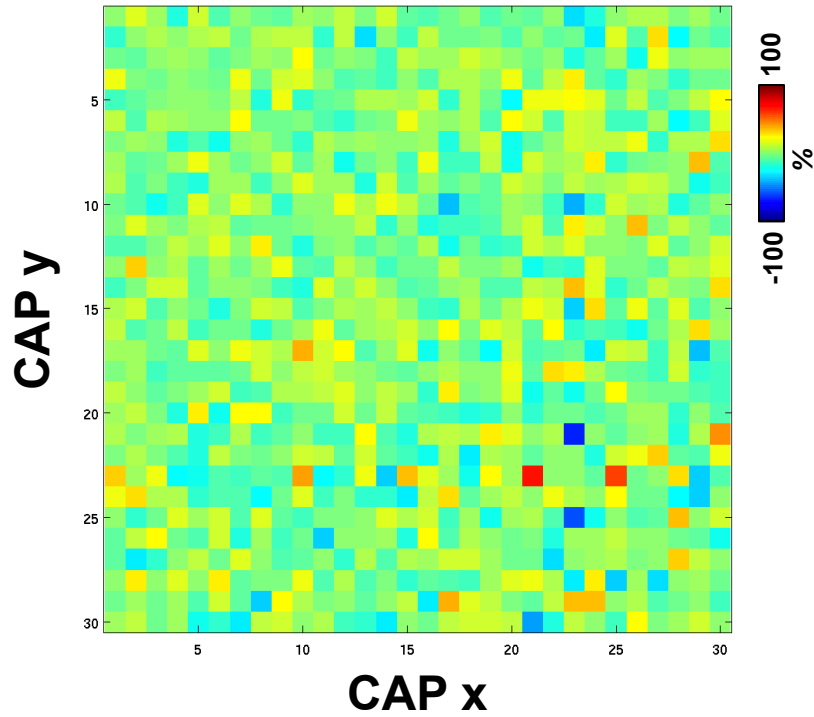


Fig. S9. Symmetric temporal relationship of CAPs. The matrix shows the difference between probabilities of seeing CAP x ahead of CAP y (within 2 TR) and of seeing CAP x behind CAP y (within 2 TR). The small values suggest a symmetric appearance of x-y and y-x sequences. We further tested whether such differences are significant under the null hypothesis that we have equal probability of seeing either of them first. The testing based on a binomial distribution model found none of these differences significant at level of 0.05 after Bonferroni correction, even for the CAP 23 – CAP 25 and CAP 21 – CAP 23 pairs that showed the highest values in the matrix.

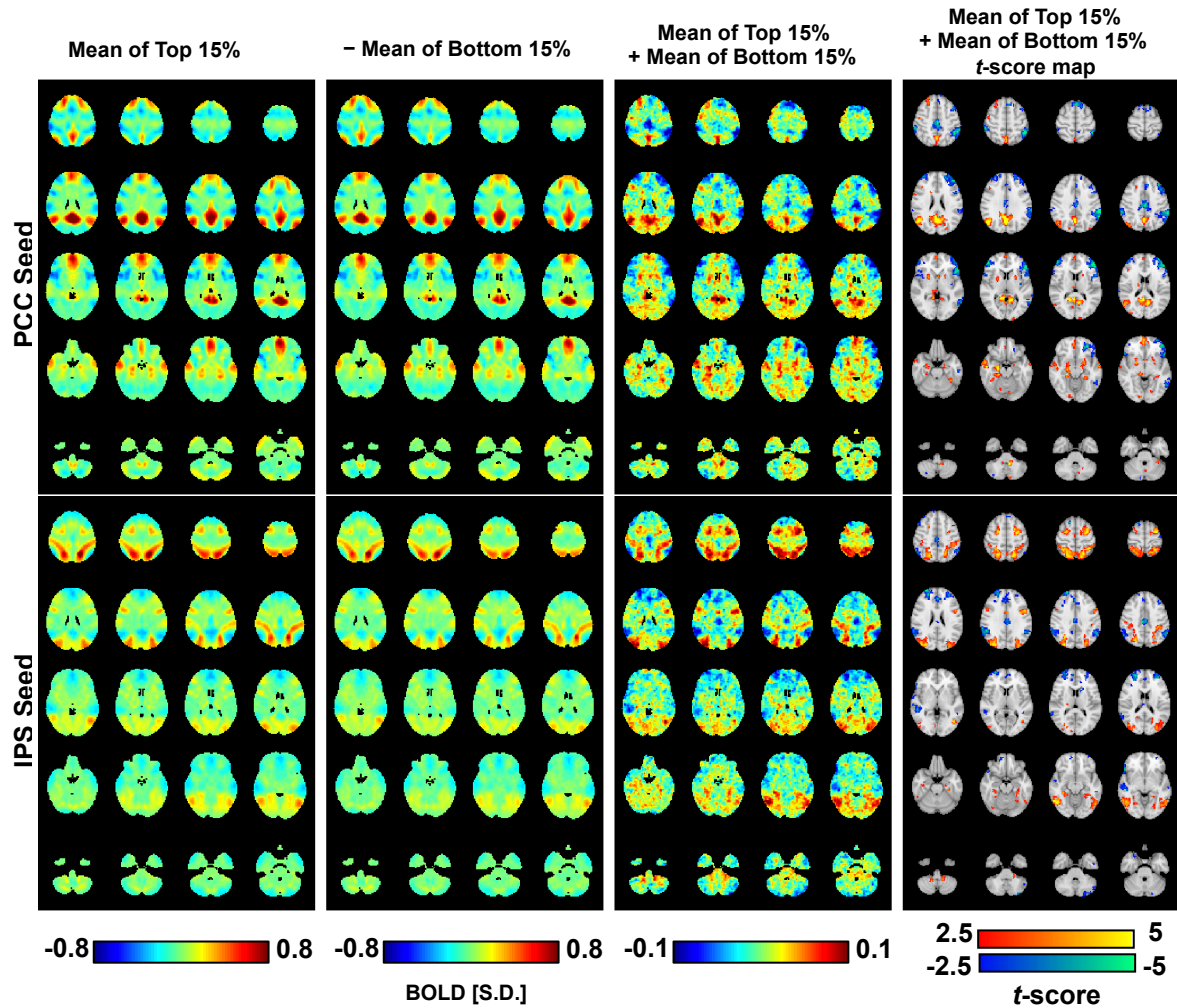


Fig. S10. A comparison of co-activation and co-deactivation patterns using 15% of the data at top and bottom ranges. The first column is the mean image of the top 15% time frames selected based on corresponding seeds (the posterior cingulate cortex, PCC; and the Intraparietal sulcus, IPS) while the second column is the mean image of the bottom 15% frames with its sign flipped; the third column is the sum of the two mean images, corresponding to the difference between the left and middle column. Although by flipping the sign, the co-deactivation shows a similar pattern as the co-activation, there is a clear difference (10~15%, note the scale in color bar) between them with distinct spatial patterns. The difference tends to be positive within seed-related regions (“task-negative” regions for PCC and “task-positive” regions for IPS) but negative in the negatively correlated regions.